

RESEARCH

Open Access



Quantitative analysis of acetylation in peste des petits ruminants virus-infected Vero cells

Xuelian Meng^{1*}, Xiangwei Wang¹, Xueliang Zhu¹, Rui Zhang², Zhidong Zhang^{2*} and Yuefeng Sun¹

Abstract

Background *Peste des petits ruminants virus* (PPRV) is a highly contagious pathogen that strongly influences the productivity of small ruminants worldwide. Acetylation is an important post-translational modification involved in regulation of multiple biological functions. However, the extent and function of acetylation in host cells during PPRV infection remains unknown.

Methods Dimethylation-labeling-based quantitative proteomic analysis of the acetylome of PPRV-infected Vero cells was performed.

Results In total, 1068 proteins with 2641 modification sites were detected in response to PPRV infection, of which 304 differentially acetylated proteins (DACPs) with 410 acetylated sites were identified (fold change < 0.83 or > 1.2 and $P < 0.05$), including 109 up-regulated and 195 down-regulated proteins. Gene Ontology (GO) classification indicated that DACPs were mostly located in the cytoplasm (43%) and participated in cellular and metabolic processes related to binding and catalytic activity. Functional enrichment indicated that the DACPs were involved in the minichromosome maintenance complex, unfolded protein binding, helicase activity. Only protein processing in endoplasmic reticulum pathway was enriched. A protein-protein interaction (PPI) network of the identified proteins further indicated that a various chaperone and ribosome processes were modulated by acetylation.

Conclusions To the best of our knowledge, this is the first study on acetylome in PPRV-infected host cell. Our findings establish an important baseline for future study on the roles of acetylation in the host response to PPRV replication and provide novel insights for understanding the molecular pathological mechanism of PPRV infection.

Keywords Acetylation, Post-translational modification, protein-protein interaction, *Peste des petits ruminants virus*

Background

Peste des petits ruminants virus (PPRV) is a highly contagious virus that profoundly diminishes the productivity of small ruminants worldwide. PPRV, belonging to the genus *Morbillivirus* in the family *Paramyxoviridae* [1], has a negative, non-segmented single-stranded RNA genome that encodes six structural proteins (nucleocapsid protein, N; phosphoprotein, P; matrix protein, M; fusion protein, F; haemagglutinin protein, H; and large polymerase protein, L) in the 3' to 5' direction and two non-structural proteins (V and C proteins). PPRV was first reported in the Ivory Coast of West Africa, in 1942

*Correspondence:

Xuelian Meng
mengxuelian@caas.cn
Zhidong Zhang
zhangzhidong@swun.edu.cn

¹State Key Laboratory for Animal Disease Control and Prevention, Key Laboratory of Animal Virology of Ministry of Agriculture, Lanzhou Veterinary Research Institute, Chinese Academy of Agricultural Sciences, Xujiaping 1, Yanchangpu, Chengguan District, Lanzhou 730046, China
²College of Animal and Veterinary Sciences, Southwest Minzu University, Chengdu, Sichuan, China



© The Author(s) 2023. **Open Access** This article is licensed under a Creative Commons Attribution 4.0 International License, which permits use, sharing, adaptation, distribution and reproduction in any medium or format, as long as you give appropriate credit to the original author(s) and the source, provide a link to the Creative Commons licence, and indicate if changes were made. The images or other third party material in this article are included in the article's Creative Commons licence, unless indicated otherwise in a credit line to the material. If material is not included in the article's Creative Commons licence and your intended use is not permitted by statutory regulation or exceeds the permitted use, you will need to obtain permission directly from the copyright holder. To view a copy of this licence, visit <http://creativecommons.org/licenses/by/4.0/>. The Creative Commons Public Domain Dedication waiver (<http://creativecommons.org/publicdomain/zero/1.0/>) applies to the data made available in this article, unless otherwise stated in a credit line to the data.

and is currently endemic in Africa, the Middle East and Asia affecting global trade and causing significant economic losses.

The interaction between host and virus is a complex dynamic competitive process. As obligate intracellular parasites, viruses depend on their ability to “hijack” host cellular functions to facilitate their replication and inhibit host antiviral defenses. In contrast, to maintain normal physiological functions, the host utilizes nonspecific and specific immune-based antiviral responses to resist viral invasion, inhibit virus replications, or eliminate virus particles. Therefore, a comprehensive understanding of the molecular mechanism underlying the interaction between the host and PPRV infection may help to further explore the mechanism of PPRV pathogenesis, as well as the development of novel alternative therapeutic approaches.

Protein post-translational modifications (PTMs) affect the functions of proteins by modulating biological processes, protein activity, cellular location and protein-protein interaction (PPI) by transferring modified groups to one or more amino acid residues. To date, more than 450 protein modifications including over 200 PTMs have been identified [2] as dynamic and reversible protein-processing events that play key roles in disease pathogenesis [3–6]. Some PTMs including phosphorylation, acetylation and succinylation potently regulate innate immunity and inflammation in response to viral infection [7, 8].

Of the 20 amino acid residues, lysine is one of the most frequent targets of covalent modifications because it can accept different types of chemical groups [9–14]. Among the lysine PTMs, lysine acetylation is widespread and one of the most well-studied PTMs in both prokaryotes and eukaryotes [2, 15–18]. Lysine acetylation is highly conserved in organisms ranging from bacteria to humans and is particularly important as it affects protein function in multiple cellular processes, including enzyme activity, chromatin structure, localization and PPIs [16, 17, 19–21]. Accumulating evidence indicates that lysine acetylation is an important molecular toggle for protein function [15, 22–24] and is a key regulatory point in mechanisms of both the host antiviral response and virus replication [25–28]. ID1 suppresses FOXO1 transcriptional activity through HDAC4-mediated deacetylation to inhibit foot-and-mouth disease virus replication [28]. RBM10, a splicing factor responsible for SAT1 exon 4 skipping, interacts with dengue viral RNA and RIG-I, and even promotes the ubiquitination of the latter, a crucial step for its activation. It indicated that RBM10 fulfills diverse pro-inflammatory and anti-viral tasks in addition to its well-documented role in the splicing regulation of apoptotic genes [29]. NP acetylation at highly conserved lysine residues affects multiple steps in the replication of

influenza A viruses [25]. Lysin acetylation at the nuclear periphery protects against herpesvirus human cytomegalovirus production by inhibiting capsid nuclear egress [26]. However, the extent and function of lysine acetylation in host cells during PPRV infection has not yet been reported.

In this study, we investigated the acetylome of Vero cells infected with PPRV. By combining dimethylation labeling, HPLC fractionation and antibody-affinity enrichment with LC-MS/MS analysis, we systematically and quantitatively compared the acetylome of Vero cells with or without PPRV infection, and calculated the regularity of sequence features around the acetylated sites. We successfully quantified 2641 lysine acetylation sites in 1068 proteins with diverse molecular functions, biological processes and subcellular localizations. Altogether, the results present the first extensive dataset on lysine acetylation in Vero cells infected with PPRV and provide novel insights into the infection mechanism of PPRV.

Methods

Cells, virus and infection

Vero cells were maintained in authors' laboratory, and cultured in DMEM medium (Sigma Aldrich, St Louis, MO, USA) supplemented with 10% fetal bovine serum, 100 IU/ml penicillin and 100 µg/ml streptomycin and incubated at 37 °C in 5% CO₂ incubator. The PPRV vaccine strain Nigeria 75/1 preserved in our laboratory was propagated and passaged in Vero cells as previously described [30]. Vero cells seeded in 6-well cell culture plates were infected with PPRV at a MOI of 0.1 or mock-infected with phosphate-buffered saline (PBS, 0.01 M, pH7.4) and incubated at 37 °C for 1 h. The MOI was estimated according to the viral titer of Vero cell line. After adsorption, the virus inoculum was removed and the fresh medium was added to the wells and incubated. In order to determine the sampling time point, the cells were harvested at 24, 48, 72 h post infection (hpi) and analyzed using western blotting and a pan anti-acetyllsine antibody (PTM-104, PTM Biolabs, Chicago, USA). Three independent biological replicates (three parallel experiments) were performed. The flow chart of the present study was shown in Fig. 1.

Protein extraction

The samples consisted of harvested infected and uninfected cells were washed twice with cold phosphate-buffered saline (PBS) and dispensed in lysis buffer (8 M urea, 1% Protease Inhibitor Cocktail, 3 µM TSA, 50 mM NAM and 2 mM EDTA) then each sample was sonicated on ice. The resulting supernatants were centrifuged at 12,000 rpm for 10 min at 4 °C to remove cellular debris. The protein concentration was determined using a BCA kit according to the manufacturer's instructions.

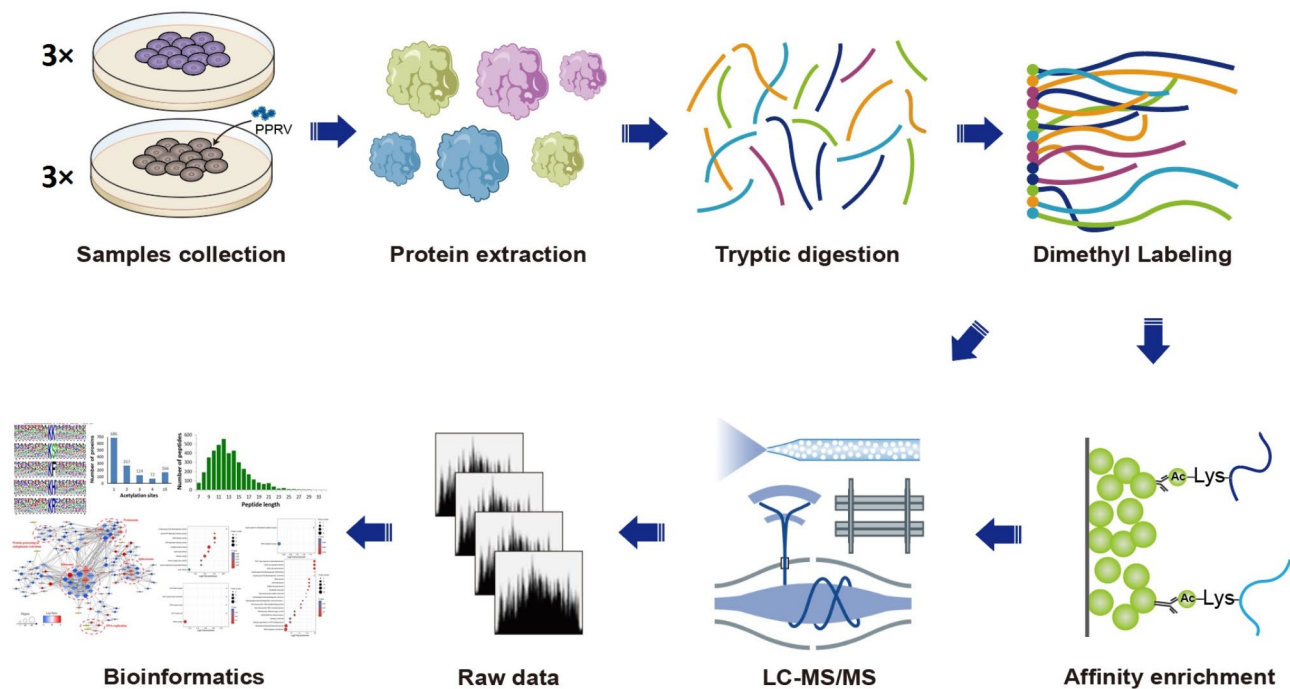


Fig. 1 Flowchart of virus infection, proteomic analysis and global mapping of acetylation in PPRV-infected Vero cells

Trypsin digestion and dimethylation labeling

The protein solution was reduced with 5 mM dithiothreitol for 30 min at 56 °C and subsequently alkylated with 11 mM iodoacetamide for 15 min at room temperature in the dark. For tryptic digestion, the protein samples were diluted with urea concentration of less than 2 M by adding 100 mM NH_4CO_3 . Finally, trypsin was added at 1:50 trypsin-to-protein mass ratio for the first digestion overnight and at 1:100 trypsin-to-protein mass ratio for a second 4 h-digestion at 37 °C. Then, peptide was desalted using Strata X C18 SPE column (Phenomenex) and vacuum-dried. Peptide samples were resuspended in 0.1 M TEAB and labeled in parallel in different tubes by adding CH_2O or CD_2O to the control and infected samples, respectively. The reactions were mixed and further treated with NaBH_3CN (sodium cyanoborohydride), incubated for 2 h at room temperature, then desalted by adding formic acid, and vacuum dried.

Enrichment for acetylated peptides

Lysine-acetylated peptides were enriched with an agarose-conjugated pan anti-acetyllysine antibody (PTM Biolabs, Hangzhou, China). In brief, dried tryptic peptides re-dissolved in NETN buffer (100 mM NaCl, 1 mM EDTA, 50 mM Tris-HCl, 0.5% NP-40, pH 8.0) were incubated with pre-washed anti-acetyllysine pan antibody-conjugated agarose beads (PTM-104, PTM Biolabs, Hangzhou, China) and incubated at 4 °C overnight with gentle shaking. Then the beads were washed four times with NETN buffer and twice with ice-cold ddH_2O . The

bound peptides were eluted three times from the beads with 0.1% trifluoroacetic acid (TFA; Sigma-Aldrich, St. Louis, USA). The eluted fractions were pooled together and vacuum-dried. The resulting peptides were desalted using C18 ZipTips (Merck Millipore, Billerica, MA, USA) according to the manufacturer's instructions and dried by vacuum centrifugation, followed by LC-MS/MS analysis.

LC-MS/MS analysis

The enriched peptides were dissolved in solvent A (0.1% Formic Acid in 2% acetonitrile (ACN)), directly loaded onto a home-made reversed-phase analytical column (1.9 μm particles, 120 Å pore, 15 cm length, 75 μm i.d.). The gradient included an increased concentration of solvent B (0.1% Formic Acid in 90% ACN) starting from 9 to 25% for 24 h, followed by 25–40% for 10 min, and reaching to 80% in 3 min, then maintained at 80% for the last 3 min on an EASY-nLC 1000 UPLC (Ultra Performance Liquid Chromatography) system at a constant flow rate of 700 nL/min.

The resulting peptides were ionized and subjected to tandem mass spectrometry (MS/MS) in Q Exactive™ Plus (Thermo Scientific) coupled online to the UPLC using NanoSpray Ionization (NSI) source. The applied electrospray voltage was 2.0 kV. Intact peptides were detected at a resolution of 70,000 with scan range of 350–1800 m/z for full MS scans in the Orbitrap. Peptides were then selected for MS/MS using NCE setting of 28 and ion fragments were detected at a resolution of 17,500. Data-dependent acquisition (DDA), which alternated between

one MS scan followed by 20 MS/MS scans, was applied for the top 20 precursor ions with 15 s dynamic exclusion. Automatic gain control (AGC) was used to prevent overfilling of the ion trap and set at 5E4, with a fixed first mass of 100 m/z.

Database searches

The protein acetylation sites identification and quantification were processed using MaxQuant search engine (v.1.5.2.8) against the *Chlorocebus sabaues* database (19,228 sequences), concatenated with a reverse database and common contaminants. Trypsin/P was specified as a cleavage enzyme allowing up to 4 missing cleavages. The mass tolerance for precursor ions was set to 20 ppm in the first search and 5 ppm in the main search, and the mass tolerance for fragment ions was set to 0.02 Da. Carbamido-methylation of cysteine (Cys) was specified as a fixed modification, and oxidation of methionine, acetylation on the protein N-terminal, and acetylation on lysine were specified as variable modifications. The false discovery rate (FDR) and the minimum score for the modified peptide were set to <1% and >40, respectively. The minimum peptide length was set to 7. All other parameters in MaxQuant were set to default values.

Bioinformatics annotation analysis

Gene Ontology (GO) annotations were derived from the UniProt-GOA database (<http://www.ebi.ac.uk/GOA/>). The proteins were classified into three categories: biological processes, cellular components and molecular function. Protein domain annotation was performed using InterProScan (<http://www.ebi.ac.uk/InterProScan/>) based on the protein sequence alignment method, and the InterPro domain database (<http://www.ebi.ac.uk/interpro/>). The Kyoto Encyclopedia of Genes and Genomes (KEGG) database (<http://www.genome.jp/kegg/>) was used to annotate and map pathways. GO, protein domain and KEGG pathway enrichment analysis were performed using DAVID Bioinformatics Resources 6.8. Wolfpsort (<https://wolfpsort.hgc.jp/>), a subcellular localization predication software was used to predict subcellular localization. Amino acid sequence motifs (within ± 10 residues of acetylated sites) were analyzed by Motif-X. Motif-based clustering analyses were also performed, and cluster membership was visualized using a heat map. Functional interaction network analysis was performed using the STRING database (v.11.0), with a high confidence threshold of 0.7 (high confidence), and visualized using Cytoscape 3.7.1.

Results

Identification of acetylated sites and proteins in PPRV-infected Vero cells

Lysine acetylation can alter the structure and function of proteins involved in diverse biological processes. To explore the acetylated host proteins or pathways involved in PPRV replication, we selected 24 hpi as the time point for quantitative proteomic analysis according to the results of western blotting (Additional file 1: Fig. S1). A combination of iTRAQ based quantitative proteomic and LC-MS/MS was used to identify acetylated proteins and acetylation sites (Fig. 1). The near-zero distribution of mass error and that the errors were predominantly <0.02 Da (Additional file 2: Fig. S2). Most of the enriched lysine-acetylated peptide lengths were in the size range from 7 to 21 amino acids (Fig. 2A), which was consistent with trypsin cutting at lysine residue sites. The mass spectrometry data have been deposited at the ProteomeXchange (<http://proteomecentral.proteomexchange.org/cgi/GetDataset>) with dataset identifier PXD025081.

In total, 3229 acetylated sites belonging to 1315 proteins were identified, of which 2641 modification sites in 1068 proteins were quantifiable (Additional file 3: Table S1). Among these quantifiable proteins, approximately 686 (52.16%) contained a single acetylation site, 267 (20.30%) included two acetylation sites, 124 (9.43%) included three acetylation sites, 72 (5.48%) included four acetylation sites, and 166 (12.62%) included five or more than five acetylation sites (Fig. 2B). A total of 107 acetylation sites were found on histone proteins, including 13 sites in H1, 12 sites in H2A, 13 sites in H2B, 9 sites in H3 and 8 sites in H4. These results provide a comprehensive overview of the acetylation events in PPRV-infected Vero cells.

Based on a threshold of 1.2-fold changes and t test $P < 0.05$ as standards, 410 acetylated sites in 304 differentially acetylated proteins (DacPs) were identified (Additional file 4: Table S2), of which 126 acetylated sites in 109 DacPs were up-regulated, and 284 acetylated sites in 195 DacPs were down-regulated (Fig. 3). Most DacPs were modified at a single acetylation site. 79 were modified at multiple lysine acetylation sites, including PDIA4 (7 sites), vimentin (6 sites), plectin (5 sites), nucleolin (NCL, 4 sites) and molecular chaperones. Heat shock proteins (Hsps), including HspA8, HspA5, HspA9, Hsp90AB1 and Hsp90B1, were acetylated at 8, 3, 2, 3 and 3 sites, respectively. Two different sites were acetylated in six paralogous subunits of chaperonin TRiC (also called CCT).

Functional, subcellular localization and COG classification of differentially acetylated proteins

To better understand the potential functions of acetylation in PPRV-infected cells, all DacPs were classified by GO analysis based on their biological process, molecular

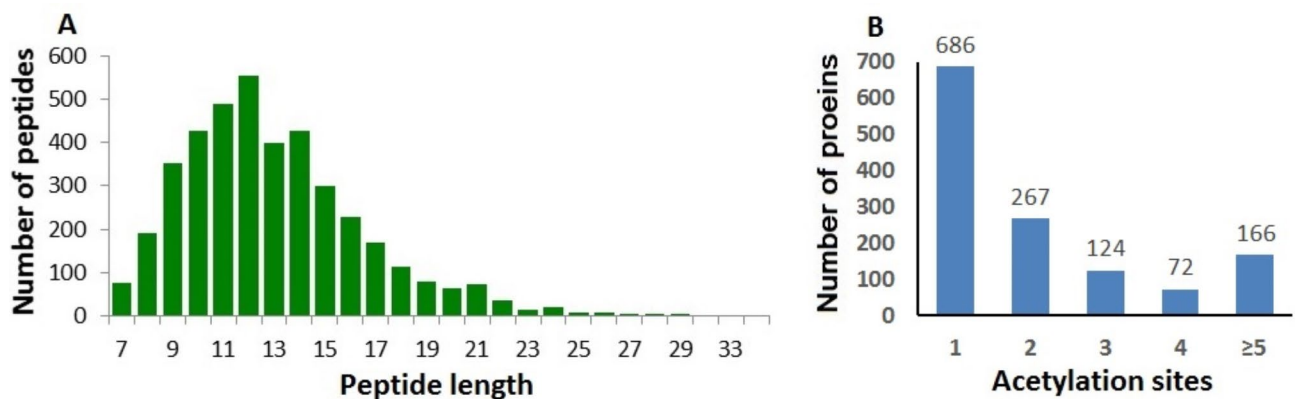


Fig. 2 The identification of acetylation proteins and sites in PPRV-infected Vero cells; **A** Peptide length distributions of acetylation profiles; **B** Summary of the acetylated proteins and sites identified

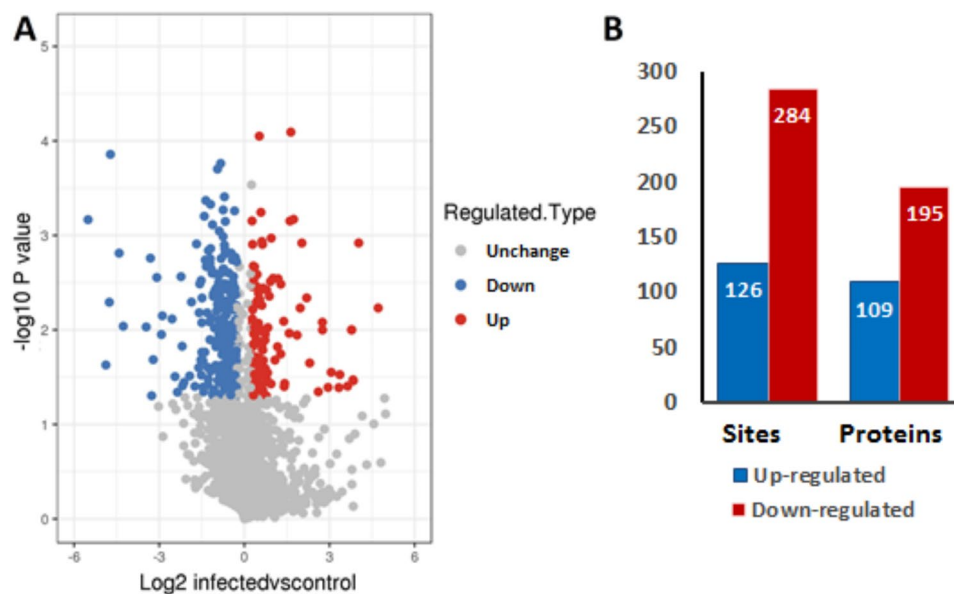


Fig. 3 Effects of PPRV on protein acetylation of Vero cells; **A** A volcano map was constructed using fold-change values and P-values to show acetylated proteins abundance in the two groups, the difference multiple (logarithmic transformation with base 2) was plotted on the abscissa and P-values (logarithmic transformation with base 10) were plotted along the longitudinal axis. Gray dots represented proteins that are not significantly differentially acetylated ($P > 0.05$). Up-regulated DACPs were presented as red dots and down-regulated DACPs were presented as blue dots; **B** Summary of the differentially acetylated proteins and sites (fold change < 0.83 or > 1.2 and $P < 0.05$)

function, subcellular localization, and COG/KOG categories (Fig. 4 & Additional file 5: Table S3).

With regard to biological processes, the acetylated-proteins were primarily associated with either cellular process (34%) or metabolism process (30%) (Fig. 4A). The classification results for molecular function indicated that DACPs were mostly involved in binding (58%) and catalytic activity (30%). Most of DACPs were distributed in the cytoplasm (43%), nucleus (25%), mitochondria (15%) or extracellular (7%) (Fig. 4B). Furthermore, based on the results of COG/KOG classification, 271 DACPs were successfully annotated into 4 categories (Fig. 4C): 39% were involved in cellular processes and signaling; 40% played roles in posttranslational modification,

protein turnover, and chaperones; 34% were associated with information storage and processing; and 67% were involved in translation, ribosomal structure and biogenesis, RNA processing and modification. All classification results of the up-regulated acetylated proteins were similar to those of the down-regulated acetylated proteins.

Motifs analysis of acetylated sites

Amino acid residues surrounding the central lysine acetylation residues have specific patterns and preferences in both eukaryotes and prokaryotes [31]. Thus, to determine the characteristics of acetylated lysine in PPRV-infected Vero cells, the conserved motif surrounding the specific acetylated sites was investigated using the Motif-X

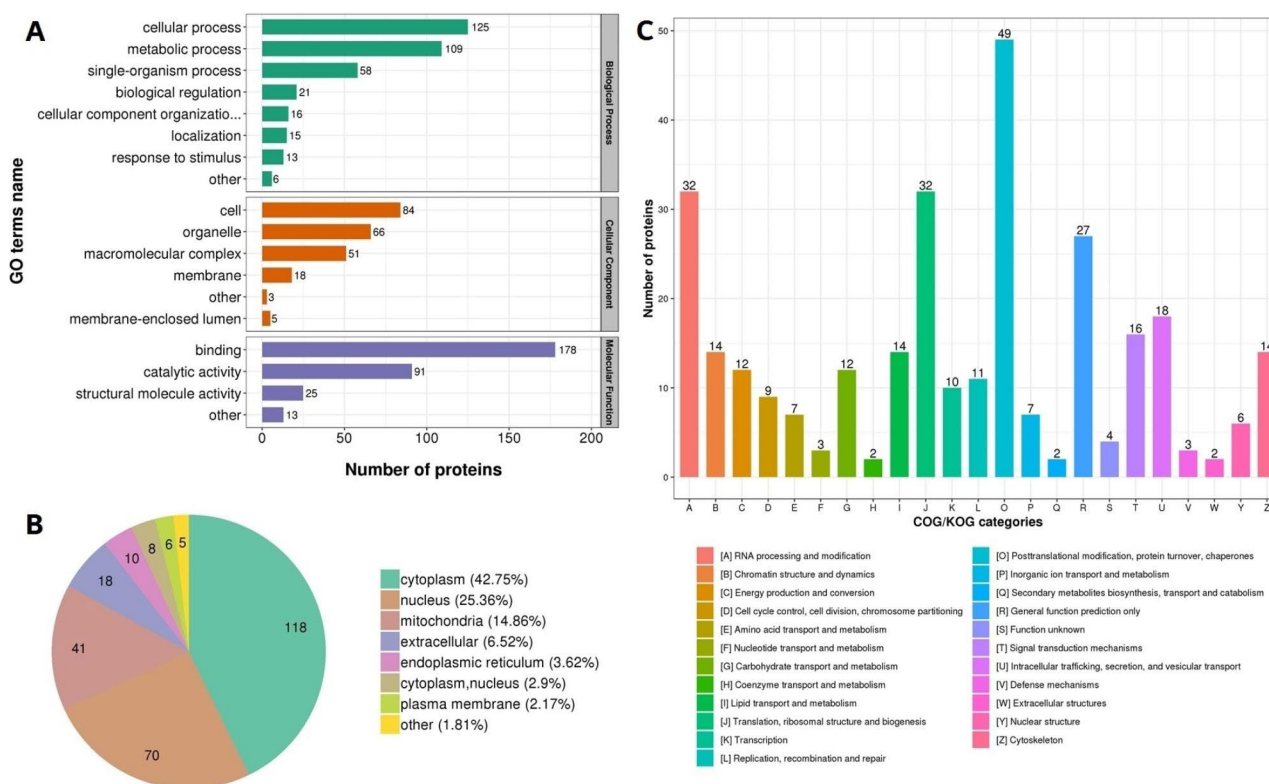


Fig. 4 Functional classification of the identified DACPs in PPRV-infected Vero cells; **A** GO classification of the identified acetylated proteins in three categories: biological process, cellular component and molecular function; **B** Subcellular localization; **C** COG/KOG classification

program with a significance threshold of $P < 0.000001$. The amino acids flanking the acetylated sites were matched to the whole size, and the motif enrichment was illustrated in the form of a heat map.

Of all the acetylated peptides, 13 significantly enriched lysine acetylation site motifs from 2489 modified sites were identified within ten amino acids upstream and downstream positions of the acetylated lysine (Fig. 5). These motifs were KacK, KacS, KacF, KacH, KacR, KacT, KacN, KacL, KacV, KacG, KacI, KacD and Kac***K (Kac: acetylated lysine; *: residue of a random amino acid; Fig. 5A). Motif enrichment was also illustrated in the form of a heat map (Fig. 5B). The 2489 modified sites accounted for 86.6% of the sites identified according to the criteria of specific amino acid sequence. There was significant enrichment of lysine (K), serine (S), phenylalanine (F), histidine (H), arginine (R), threonine (T), asparagine (N), leucine (L), valine (V), glycine (G), and isoleucine (I) at position +1 (75.4%, Fig. 5C). The first motif was remarkably conserved, and acetylated peptides with this motif accounted for approximately 15.7% of all identified acetylated peptides.

Enrichment analysis of differentially acetylated proteins

In order to further explore the functions of the acetylated proteins during PPRV infection, GO enrichment (cellular

component, biological process and molecular function), KEGG and protein domain analysis were performed for all identified proteins with differentially acetylated sites (Fig. 6 & Additional file 6: Table S4).

In the molecular function category, unfolded protein binding and helicase activity were found to be significantly enriched (Fig. 6A). Only two enriched biological processes (single-organism carbohydrate catabolic and DNA metabolic processes) were identified (Fig. 6B). The most enriched cellular component was minichromosome maintenance (MCM) complex (Fig. 6C). The KEGG database was used to identify pathways associated with the DACPs. 17 DACPs were involved in protein processing in endoplasmic reticulum (ER), and 12 of which were down-regulated. Protein domain analysis showed that a large proportion of DACPs were associated with the nucleotide-binding domain, RNA recognition motif domain, GroEL-like domain, TCP-1-like chaperonin intermediate domain, MCM domain and DEAD/DEAH box helicase domain (Fig. 6D).

Protein-protein interaction network analysis of differentially acetylated proteins

To better understand how acetylation regulates diverse metabolic processes and cellular functions, we assembled PPI networks of the identified modified proteins. In total,

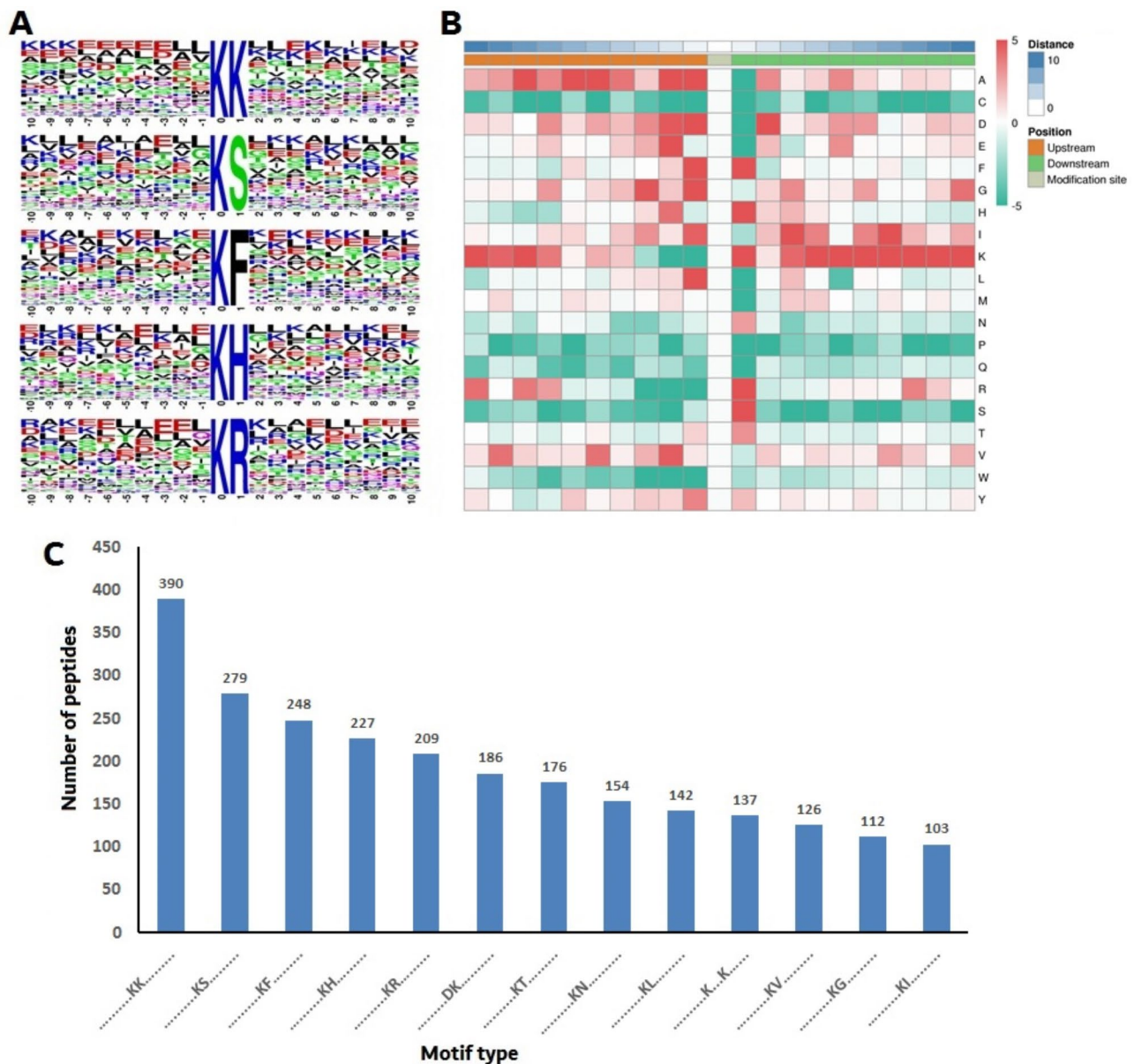


Fig. 5 Characterization of acetylated peptides; **A** Probability sequence motifs of acetylation sites consisting of 20 residues surrounding the targeted lysine residue using Motif-X. thirteen significantly enriched acetylation site motifs were identified; **B** Heat map showing upstream (red) or downstream (green) of amino acid compositions around the acetylated lysine site (10 amino acids upstream and downstream of the acetylated lysine site); **C** Number of identified peptides possessing an acetylated lysine in each motif

147 DAcPs were mapped to the protein network database. A global network graph of these interactions was shown in Fig. 7 and Additional file 7: Table S5. As shown in Fig. 7, five highly connected subnetworks, namely, ribosomes, proteasomes, spliceosomes, protein processing in the ER, and DNA replication of DAcPs, were enriched. In the first subnetwork, 19 proteins with 96 Kac sites and 484 direct physical interactions participated in the ribosomal interaction, suggesting that they play key roles in protein synthesis. The second subnetwork is related to the 26 S proteasome and chaperone, and comprised 14

proteins with 75 Kac sites and 184 direct physical interactions. Among the 14 proteins, six subunits of the 26 S proteasome and five paralogous subunits of chaperonin containing the T-complex polypeptide-1 (CCT, also called TRiC) were identified as DAcPs in PPRV infection: proteasome 20 S subunit (PSMA4, PSMA5, and PSMB3), proteasome 19 S subunits (PSMC5, PSMD11 and PSMD13) and CCT subunit (CCT3, CCT4, CCT5, CCT6A and CCT7). Moreover, in the ribosome and proteasome subnetworks, a tight PPI network including 8 up-regulated proteins and 25 down-regulated proteins,

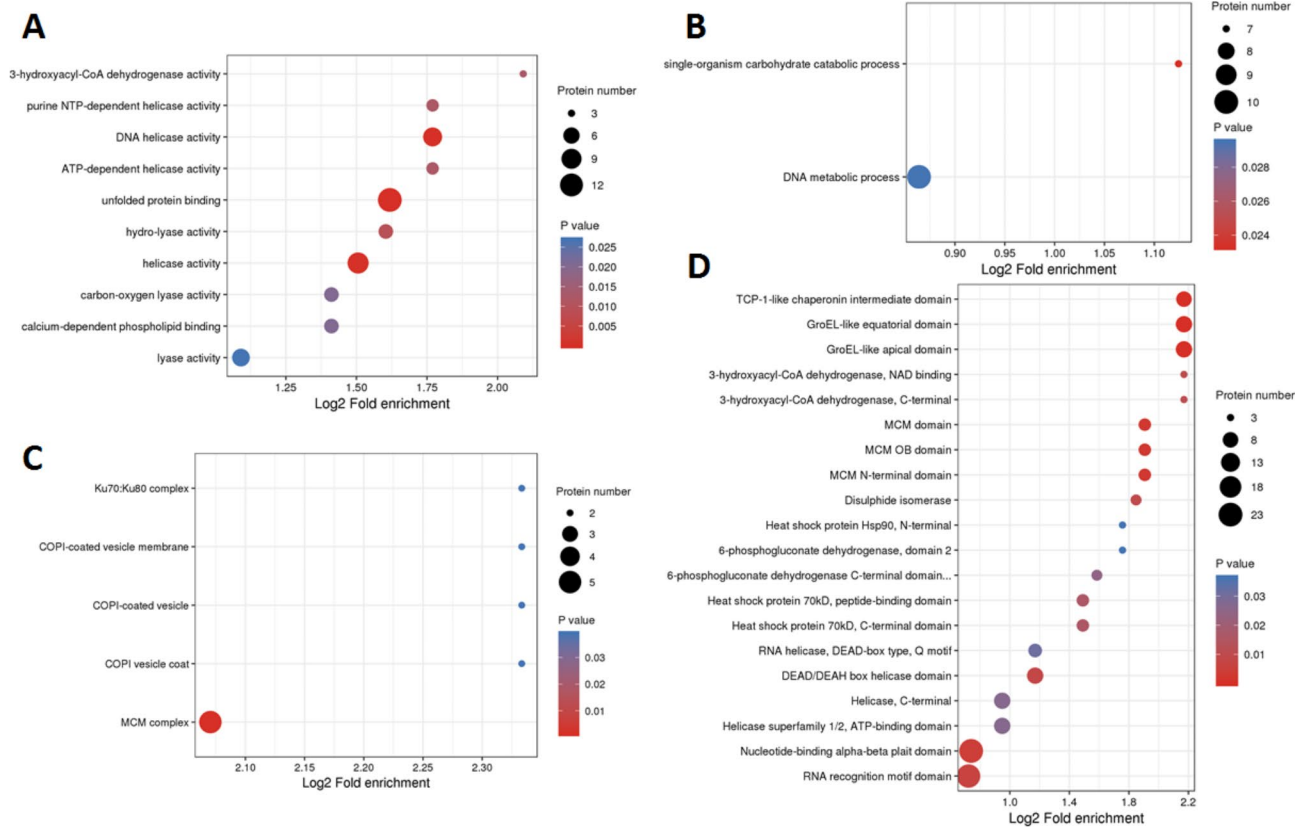


Fig. 6 GO and domain enrichments of DACPs; **A** Molecular function; **B** Biological process; **C** Cellular component **D** Protein domain. The x-axis was the rich factor which means the proportion of DACPs in total proteins. The y-axis was the protein functional classification. Different colors of plots indicated different P values. Plot diameter represented DACPs numbers in a GO term

was significantly enriched. Most proteins in the PPI network contained more than two acetylated sites. Overall, these results suggest complex interactions among acetylated proteins that may control the disease response or resistance during PPRV infection.

Discussion

Pathogen infection can regulate biological processes of the host at various levels that can lead to major changes in the proteome, involved at transcriptional, post-transcriptional, translational, and post-translational levels. As a widespread PTM, lysine acetylation plays central roles in regulating multiple biological processes, particularly metabolism [5]. Recently, increasing instances of protein acetylation on lysine residues have been reported. Accumulating evidence suggests that lysine acetylation is a key molecular toggle for host antiviral responses and virus replication either directly or indirectly [25, 26, 32]. Despite these findings, protein acetylation remains an understudied aspect of viral infections due to the lack of knowledge regarding its temporal regulation during infection.

Although comparative transcriptome and proteomic profiling has been performed in bone marrow-derived

dendritic cells (BMDCs) and peripheral blood mononuclear cells (PBMCs) stimulated with PPRV [33–35], little is known about lysine acetylation in cells infected with PPRV. In this study, we used acetylome analysis approaches based on affinity purification and LC–MS/MS to elucidate the effects of PPRV infection on the protein lysine acetylation profiles of Vero cells to gain insight into PPRV pathogenesis. This is the first systematic analysis of acetylation in Vero cells infected with PPRV, providing an important starting point for functional studies of acetylated proteins in response to PPRV infection. Among the DACPs identified, vimentin and NCL were modified at multiple lysine acetylation sites. Vimentin, one of the most widely expressed intermediate filament proteins, can facilitate viral internalization, entry and replication by interacting with the proteins of porcine reproductive and respiratory syndrome virus (PRRSV), Japanese encephalitis virus, parvovirus, enterovirus 71, SARS-CoV, Bluetongue virus, dengue virus and transmissible gastroenteritis virus [36–44]. Rearrangement of cytosolic vimentin and the formation of vimentin cages around the viral factories in African swine fever virus and vaccinia virus infection were beneficial for preventing the movement of viral components into the cytoplasm

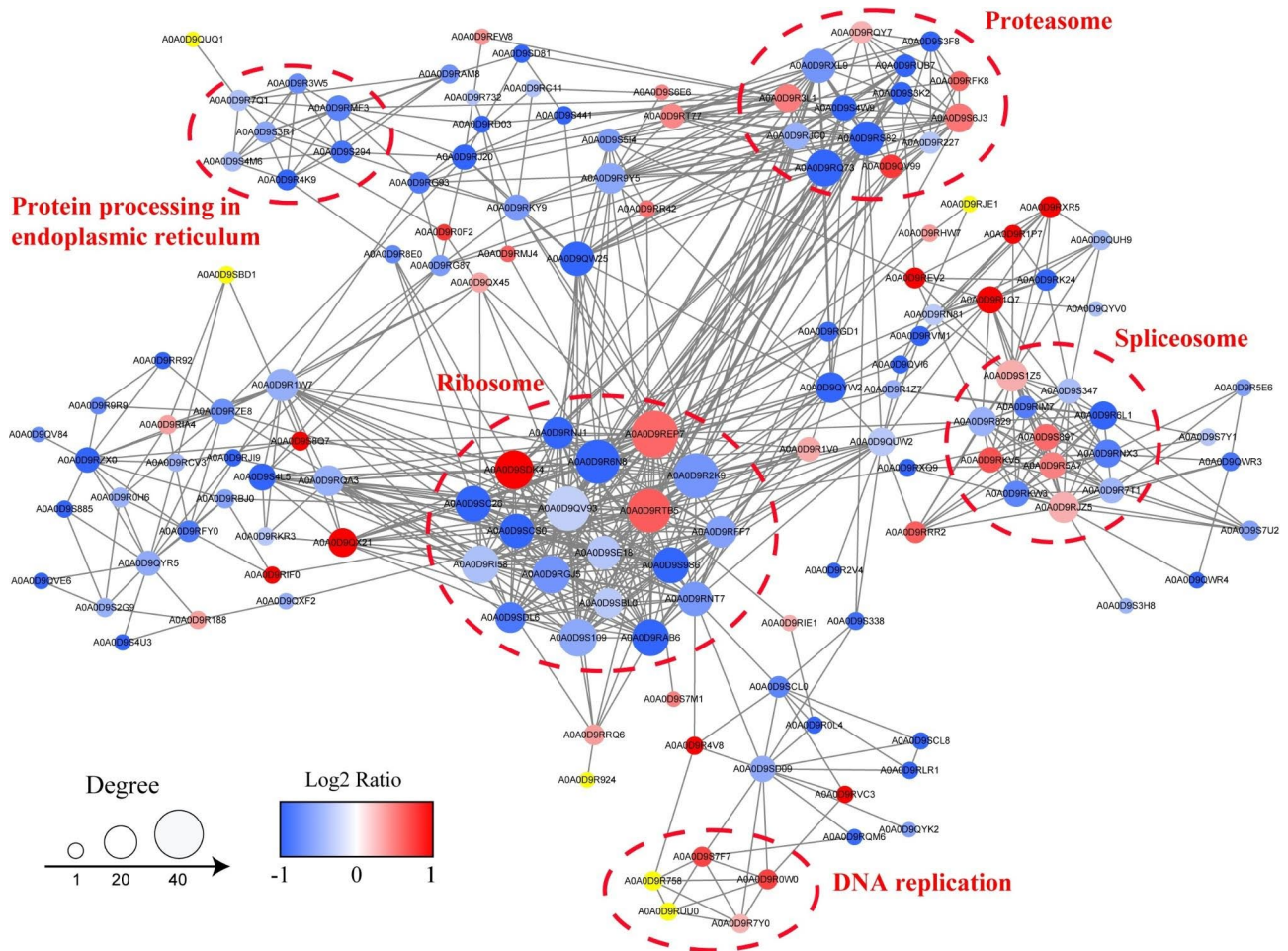


Fig. 7 The protein-protein interaction network of DACPs. Each node represented a protein, and each line indicates an interaction. Node colors represent fold change, and circle size represents the numbers of DACPs. Red indicates upregulated DACPs and blue indicates downregulated DACPs

and contributing to efficient assembly and replication of the virus [45, 46]. NCL also plays important roles in the entry, replication and intracellular transport of several viruses. Changes in NCL localization in virus-infected cells have been reported. NCL interacts with PPRV N protein and indirectly inhibits PPRV growth by stimulating the interferon (IFN) pathway [47]. In contrast, NCL facilitates the entry of influenza A viruses and enterovirus (EV)71 [48, 49]. Acetylated NCL is present in speckle structures in the nucleoplasm and co-localizes with the splicing factor SC35, suggesting that NCL is involved in pre-mRNA synthesis or metabolism [50]. Interestingly, differentially expressed DACPs were rare in PPRV-infected cells. These results suggest that the roles of acetylated proteins in PPRV entry and replication are determined by their acetylation levels.

By assessing enriched motifs in the acetylated peptides, we found that the acetylation sites identified in this study had similar sequence motifs to those in the previous reports [26, 51, 52]. We also observed that the residues flanking acetylation sites were highly enriched in

lysine at the +1 position, and frequently contained K, H and R amino acids. These results indicated that the lysine residue of a polypeptide with a K, H or R amino acid at the +1 position is the preferred substrate for lysine acetyltransferase.

GO functional classification analysis showed that many of the identified acetylated proteins in PPRV-infected cells were related to the MCM complex. The MCM complex is required for successful viral genome replication [53]. The complex composed of MCM2 to MCM7 (MCM2–7) is a part of the viral chromatin at the replication origin in the terminal repeat region, unwinds DNA to initiate replication and acts as a helicase on elongating DNA [54, 55]. However, acetylated MCM3 inhibits the initiation of DNA replication and cell cycle progression [56]. The ER is critical for protein synthesis and maturation and relies on many molecular chaperones that assist in protein folding and assembly. Virus infection can alter ER and activate the unfolded-protein response to facilitate viral replication [57, 58]. The CCT chaperonin mediates protein folding

and is essential for the assembly of functional viral replicons. CCT, a molecular chaperonin [59, 60] involved in synergistic immunity [61], apoptosis [62, 63], and cell-cycle regulation [64], mediates protein folding and is essential for the assembly of functional viral replicons. Recently, an increasing number of studies have reported that molecular chaperones play an important role in the life cycle of viruses, including viral entry, replication, transcription, translation, virion assembly, and even viral cell-cell movement [65–69]. In the present study, two different sites were acetylated in six paralogous subunits of CCT, and the acetylation levels of these CCT subunits were decreased in PPRV-infected cells, suggesting that an alteration of transcriptional response triggered by chaperones has happened, which may be able to alter PPRV infection. Based on the results of this study, acetylation of chaperonins and cytoskeletal proteins may play a vital role in viral infection; however, the relationship between PPRV infection and DACPs requires further investigation. A comprehensive study on the relationship between PPRV and these chaperones will open new directions to understand of pathogenesis, prevention and control of PPRV infection.

PPIs are critical for various biological processes. This study provides the first global PPI network of acetylated proteins induced by PPRV infection. Various cellular interactions are modulated at the acetylation level upon viral infection. Indeed, we identified subnetworks of ribosomes and proteasomes enriched in this study, indicating a critical role of these acetylated proteins in response to PPRV infection. The ubiquitin-proteasome system (UPS) regulates the expression levels of cellular proteins by ubiquitination of protein substrates followed by their degradation via the proteasome. Viruses subvert or manipulate this cellular machinery to favor viral propagation and to evade the host immune response. The UPS participates in viral propagation and acts as a double-edged sword in viral pathogenesis [70–72]. 26 S proteasome is a major molecular complex responsible for protein degradation in eukaryotes. The acetylation levels of four UPS-linked proteins (PSMA4, PSMA5, PSMC5 and PSMD13) identified as DACPs following PPRV infection were up-regulated, suggesting that viral proteins may be degraded by UPS to limit PPRV infection. The proteasome subnetwork is consistent with KEGG analysis. Mutual corroboration between the results of subnetwork proteasome and KEGG pathway enrichment confirmed the reliability of analysis.

Histone modification is a typical epigenetic modification. Increasing evidence has indicated that histone acetylation plays an important role in virus infection. Several previous studies have reported virus-induced changes in histone lysine acetylation sites, such as adenovirus [73], Borna disease virus [24, 74], Influenza virus [23, 75], HIV

[76], Zaire Ebolavirus [77], bovine herpesvirus [78], and parvovirus [79]. In this study, nine histone lysine acetylation sites were significantly differentially regulated, eight of which were down-regulated. This result hints that histone acetylation modification may also exert certain functions in Vero cells upon PPRV infection. Intensive investigations are required to explore the precise biological function of these acetylated proteins in PPRV infection.

Conclusions

In summary, our findings provide quantitative profiling of the acetylome of PPRV-infected Vero cells. We identified 304 proteins with 410 acetylation sites, that were significantly differentially acetylated in response to PPRV infection. These DACPs primarily participated in carbohydrate catabolism and DNA metabolism, suggesting that intracellular activities are extensively altered after PPRV infection. The PPI network further indicated that various chaperones and ribosomal processes were modulated by acetylation. To the best of our knowledge, this is the first study of acetylome of Vero cells infected with PPRV. This work provides an important starting point for future studies on the acetylated proteins involved in the host response to PPRV.

Abbreviations

PPR	<i>Peste des petits ruminants</i>
PPRV	<i>Peste des petits ruminants virus</i>
DACPs	differentially acetylated proteins
PPI	Protein-protein interaction
PTM	Protein post-translational modification
GO	Gene Ontology
KEGG	the Kyoto Encyclopedia of Genes and Genomes
Kac	acetylated lysine
CCT	chaperonin containing T-complex polypeptide-1

Supplementary Information

The online version contains supplementary material available at <https://doi.org/10.1186/s12985-023-02200-1>.

Additional file 1: Figure S1. Western blotting with an anti-pan acetyl-lysine antibody in response to PPRV infection in Vero cell

Additional file 2: Figure S2. A Mass error of all identified peptides; **B** Pearson's correlation of protein quantitation

Additional file 3: Tables S1. Quantitative acetylated sites on proteins

Additional file 4: Tables S2. Summary of differentially quantified acetylated sites and proteins in different groups

Additional file 5: Tables S3. Classification of differentially acetylated proteins

Additional file 6: Tables S4. Enrichment of differentially acetylated proteins

Additional file 7: Tables S5. The identified acetylated proteins used for PPI

Acknowledgements

All authors would like to thank Dr. Shuai Wang and Alfred Niyokwishimira for helpful language modification and thanked Jingjie PTM BioLab (Hangzhou) Co. Inc for providing technical support.

Authors' contributions

XML, XWW wrote the manuscript; ZDZ, YFS revised the manuscript; XML developed the study design; XLZ, RZ prepared the materials. XML, XWW analyzed the bioinformatics results. All authors read and approved the final manuscript.

Funding

This work is supported by the Agricultural Science and Technology Innovation Program (CAAS-ASTIP-2016-LVRI-05).

Data Availability

Not applicable.

Declaration

Competing interests

The authors declare no competing interests.

Ethics approval and consent to participate

Not applicable.

Consent for publication

Not applicable.

Received: 6 May 2022 / Accepted: 4 October 2023

Published online: 10 October 2023

References

1. Baron MD, Diallo A, Lancelot R, Libeau G. Peste des Petits Ruminants Virus. *Adv Virus Res.* 2016;95:1–42. <https://doi.org/10.1016/bs.avir.2016.02.001>.
2. Zhen S, Deng X, Wang J, Zhu G, Cao H, Yuan L, Yan Y. First Comprehensive Proteome analyses of lysine Acetylation and Succinylation in Seedling Leaves of *Brachypodium distachyon* L. *Sci Rep.* 2016;6:31576. <https://doi.org/10.1038/srep31576>.
3. Zhang Z, Tan M, Xie Z, Dai L, Chen Y, Zhao Y. Identification of lysine succinylation as a new post-translational modification. *Nat Chem Biol.* 2011;7:58–63. <https://doi.org/10.1038/nchembio.495>.
4. Chen L, Keppler OT, Scholz C. Post-translational modification-based regulation of HIV replication. *Front Microbiol.* 2018;9:2131. <https://doi.org/10.3389/fmicb.2018.02131>.
5. Choudhary C, Kumar C, Gnad F, Nielsen ML, Rehman M, Walther TC, Olsen JV, Mann M. Lysine acetylation targets protein complexes and co-regulates major cellular functions. *Science.* 2009;325:834–40. <https://doi.org/10.1126/science.1175371>.
6. Yang F. Post-translational modification control of HBV Biological processes. *Front Microbiol.* 2018;9:2661. <https://doi.org/10.3389/fmicb.2018.02661>.
7. Liu J, Qian C, Cao X. Post-translational modification control of Innate Immunity. *Immunity.* 2016;45:15–30. <https://doi.org/10.1016/j.immuni.2016.06.020>.
8. Zhou Y, He C, Wang L, Ge B. Post-translational regulation of antiviral innate signaling. *Eur J Immunol.* 2017;47:1414–26. <https://doi.org/10.1002/eji.201746959>.
9. Zhang K, Chen Y, Zhang Z, Zhao Y. Identification and verification of lysine propionylation and butyrylation in yeast core histones using PTMap software. *J Proteome Res.* 2009;8:900–6. <https://doi.org/10.1021/pr8005155>.
10. Zhang J, Sprung R, Pei J, Tan X, Kim S, Zhu H, Liu CF, Grishin NV, Zhao Y. Lysine acetylation is a highly abundant and evolutionarily conserved modification in *Escherichia coli*. *Mol Cell Proteomics.* 2009;8:215–25. <https://doi.org/10.1074/mcp.M800187-MCP200>.
11. Peng C, Lu Z, Xie Z, Cheng Z, Chen Y, Tan M, Luo H, Zhang Y, He W, Yang K, Zwaans BM, Tishkoff D, Ho L, Lombard D, He TC, Dai J, Verdin E, Ye Y, Zhao Y. The first identification of lysine malonylation substrates and its regulatory enzyme. *Mol Cell Proteomics.* 2011;10:M111012658. <https://doi.org/10.1074/mcp.M111.012658>.
12. Mattioli F, Sixma TK. Lysine-targeting specificity in ubiquitin and ubiquitin-like modification pathways. *Nat Struct Mol Biol.* 2014;21:308–16. <https://doi.org/10.1038/nsmb.2792>.
13. Tan M, Luo H, Lee S, Jin F, Yang JS, Montellier E, Buchou T, Cheng Z, Rouseaux S, Rajagopal N, Lu Z, Ye Z, Zhu Q, Wysocka J, Ye Y, Khochbin S, Ren B, Zhao Y. Identification of 67 histone marks and histone lysine crotonylation as a new type of histone modification. *Cell.* 2011;146:1016–28. <https://doi.org/10.1016/j.cell.2011.08.008>.
14. Hirshey MD, Zhao Y. Metabolic regulation by lysine Malonylation, Succinylation, and glutarylation. *Mol Cell Proteomics.* 2015;14:2308–15. <https://doi.org/10.1074/mcp.R114.046664>.
15. Kim GW, Yang XJ. Comprehensive lysine acetylomes emerging from bacteria to humans. *Trends Biochem Sci.* 2011;36:211–20. <https://doi.org/10.1016/j.tibs.2010.10.001>.
16. Kwon OK, Kim S, Lee S. Global proteomic analysis of lysine acetylation in zebrafish (*Danio rerio*) embryos. *Electrophoresis.* 2016;37:3137–45. <https://doi.org/10.1002/elps.201600210>.
17. Meng Q, Liu P, Wang J, Wang Y, Hou L, Gu W, Wang W. Systematic analysis of the lysine acetylome of the pathogenic bacterium *Spiroplasma eriocheiris* reveals acetylated proteins related to metabolism and helical structure. *J Proteom.* 2016;148:159–69. <https://doi.org/10.1016/j.jprot.2016.08.001>.
18. Zhou H, Finkemeier I, Guan W, Tossounian MA, Wei B, Young D, Huang J, Messens J, Yang X, Zhu J, Wilson MH, Shen W, Xie Y, Foyer CH. Oxidative stress-triggered interactions between the succinyl- and acetyl-proteomes of rice leaves. *Plant Cell Environ.* 2018;41:1139–53. <https://doi.org/10.1111/pce.13100>.
19. Liu Z, Cao J, Gao X, Zhou Y, Wen L, Yang X, Yao X, Ren J, Xue Y. CPLA 1.0: an integrated database of protein lysine acetylation. *Nucleic Acids Res.* 2011;39:D1029–34. <https://doi.org/10.1093/nar/gkq939>.
20. Kwon OK, Sim J, Kim SJ, Oh HR, Nam DH, Lee S. Global proteomic analysis of protein acetylation affecting metabolic regulation in *Daphnia pulex*. *Biochimie.* 2016;121:219–27. <https://doi.org/10.1016/j.biochi.2015.12.007>.
21. Cheng J, Yang H, Fang J, Ma L, Gong R, Wang P, Li Z, Xu Y. Molecular mechanism for USP7-mediated DNMT1 stabilization by acetylation. *Nat Commun.* 2015;6:7023. <https://doi.org/10.1038/ncomms8023>.
22. Feng Q, Su Z, Song S, Chiu H, Zhang B, Yi L, Tian M, Wang H. Histone deacetylase inhibitors suppress RSV infection and alleviate virus-induced airway inflammation. *Int J Mol Med.* 2016;38:812–22. <https://doi.org/10.3892/ijmm.2016.2691>.
23. Zhao D, Fukuyama S, Sakai-Tagawa Y, Takashita E, Shoemaker JE, Kawaoka Y. C646, a Novel p300/CREB-Binding protein-specific inhibitor of histone acetyltransferase, attenuates influenza a virus infection. *Antimicrob Agents Chemother.* 2015;60:1902–6. <https://doi.org/10.1128/AAC.02055-15>.
24. Liu X, Zhao L, Yang Y, Bode L, Huang H, Liu C, Huang R, Zhang L, Wang X, Liu S, Zhou J, Li X, He T, Cheng Z, Xie P. Human borna disease virus infection impacts host proteome and histone lysine acetylation in human oligodendroglia cells. *Virology.* 2014;464–465:196–205. <https://doi.org/10.1016/j.virol.2014.06.040>.
25. Giese S, Ciminski K, Bolte H, Moreira EA, Lakdawala S, Hu Z, David Q, Kolesnikova L, Gotz V, Zhao Y, Dengjel J, Chin YE, Xu K, Schwemmler M. Role of influenza a virus NP acetylation on viral growth and replication. *Nat Commun.* 2017;8:1259. <https://doi.org/10.1038/s41467-017-01112-3>.
26. Murray LA, Sheng X, Cristea IM. Orchestration of protein acetylation as a toggle for cellular defense and virus replication. *Nat Commun.* 2018;9:4967. <https://doi.org/10.1038/s41467-018-07179-w>.
27. Yang Q, Tang J, Pei R, Gao X, Guo J, Xu C, Wang Y, Wang Q, Wu C, Zhou Y, Hu X, Zhao H, Chen X, Chen J. Host HDAC4 regulates the antiviral response by inhibiting the phosphorylation of IRF3. *J Mol Cell Biol.* 2019;11:158–69. <https://doi.org/10.1093/jmcb/mjy035>.
28. Ren T, Chen H, Liu X, Wang Y, Fan A, Qi L, Pan L, Bai W, Zhang Y, Sun Y. ID1 inhibits foot-and-mouth disease virus replication via targeting of interferon pathways. *FEBS J.* 2021;288:4364–81. <https://doi.org/10.1111/febs.15725>.
29. Pozzi B, Bragado L, Mammi P, Torti MF, Gaioli N, Gebhard LG, Garcia Sola ME, Vaz-Drago R, Iglesias NG, Garcia CC, Gamarnik AV, Srebrow A. Dengue virus targets RBM10 deregulating host cell splicing and innate immune response. *Nucleic Acids Res.* 2020;48:6824–38. <https://doi.org/10.1093/nar/gkaa340>.
30. Meng X, Dou Y, Cai X. Ultrastructural features of PPRV infection in Vero cells. *Viol Sin.* 2014;29:311–3. <https://doi.org/10.1007/s12250-014-3494-y>.
31. Zhou X, Qian G, Yi X, Li X, Liu W. Systematic analysis of the lysine acetylome in *Candida albicans*. *J Proteome Res.* 2016;15:2525–36. <https://doi.org/10.1021/acs.jproteome.6b00052>.

32. Wei ZQ, Zhang YH, Ke CZ, Chen HX, Ren P, He YL, Hu P, Ma DQ, Luo J, Meng ZJ. Curcumin inhibits hepatitis B virus infection by down-regulating cccDNA-bound histone acetylation. *World J Gastroenterol*. 2017;23:6252–60. <https://doi.org/10.3748/wjg.v23.i34.6252>.
33. Manjunath S, Mishra BP, Mishra B, Sahoo AP, Tiwari AK, Rajak KK, Muthuchelvan D, Saxena S, Santra L, Sahu AR, Wani SA, Singh RP, Singh YP, Pandey A, Kanchan S, Singh RK, Kumar GR, Janga SC. Comparative and temporal transcriptome analysis of peste des petits ruminants virus infected goat peripheral blood mononuclear cells. *Virus Res*. 2017;229:28–40. <https://doi.org/10.1016/j.virusres.2016.12.014>.
34. Li L, Wu J, Cao X, Zhou J, Yin S, Yang S, Feng Q, Du P, Liu Y, Shang Y, Liu X. Proteomic analysis of murine bone marrow derived dendritic cells in response to peste des petits ruminants virus. *Res Vet Sci*. 2019;125:195–204. <https://doi.org/10.1016/j.rvsc.2019.06.011>.
35. Li L, Wu J, Liu D, Du G, Liu Y, Shang Y, Liu X. Transcriptional profiles of murine bone marrow-derived dendritic cells in response to Peste des Petits Ruminants Virus. *Vet Sci*. 2019;6. <https://doi.org/10.3390/vetsci6040095>.
36. Kim JK, Fahad AM, Shanmukhappa K, Kapil S. Defining the cellular target(s) of porcine reproductive and respiratory syndrome virus blocking monoclonal antibody 7G10. *J Virol*. 2006;80:689–96. <https://doi.org/10.1128/JVI.80.2.689-696.2006>.
37. Das S, Ravi V, Desai A. Japanese encephalitis virus interacts with vimentin to facilitate its entry into porcine kidney cell line. *Virus Res*. 2011;160:404–8. <https://doi.org/10.1016/j.virusres.2011.06.001>.
38. Du N, Cong H, Tian H, Zhang H, Zhang W, Song L, Tien P. Cell surface vimentin is an attachment receptor for enterovirus 71. *J Virol*. 2014;88:5816–33. <https://doi.org/10.1128/JVI.03826-13>.
39. Yu YT, Chien SC, Chen IY, Lai CT, Tsay YG, Chang SC, Chang MF. Surface vimentin is critical for the cell entry of SARS-CoV. *J Biomed Sci*. 2016;23:14. <https://doi.org/10.1186/s12929-016-0234-7>.
40. Bhattacharya B, Noad RJ, Roy P. Interaction between Bluetongue virus outer capsid protein VP2 and vimentin is necessary for virus egress. *Virology*. 2007;47. <https://doi.org/10.1186/1743-422X-47>.
41. Chen W, Gao N, Wang JL, Tian YP, Chen ZT, An J. Vimentin is required for dengue virus serotype 2 infection but microtubules are not necessary for this process. *Arch Virol*. 2008;153:1777–81. <https://doi.org/10.1007/s00705-008-0183-x>.
42. Fay N, Pante N. The intermediate filament network protein, vimentin, is required for parvoviral infection. *Virology*. 2013;444:181–90. <https://doi.org/10.1016/j.virol.2013.06.009>.
43. Teo CS, Chu JJ. Cellular vimentin regulates construction of dengue virus replication complexes through interaction with NS4A protein. *J Virol*. 2014;88:1897–913. <https://doi.org/10.1128/JVI.01249-13>.
44. Zhang X, Shi H, Chen J, Shi D, Dong H, Feng L. Identification of the interaction between vimentin and nucleocapsid protein of transmissible gastroenteritis virus. *Virus Res*. 2015;200:56–63. <https://doi.org/10.1016/j.virusres.2014.12.013>.
45. Risco C, Rodriguez JR, Lopez-Iglesias C, Carrascosa JL, Esteban M, Rodriguez D. Endoplasmic reticulum-golgi intermediate compartment membranes and vimentin filaments participate in vaccinia virus assembly. *J Virol*. 2002;76:1839–55. <https://doi.org/10.1128/jvi.76.4.1839-1855.2002>.
46. Stefanovic S, Windsor M, Nagata KI, Inagaki M, Wileman T. Vimentin rearrangement during african swine fever virus infection involves retrograde transport along microtubules and phosphorylation of vimentin by calcium calmodulin kinase II. *J Virol*. 2005;79:11766–75. <https://doi.org/10.1128/JVI.79.18.11766-11775.2005>.
47. Dong D, Zhu S, Miao Q, Zhu J, Tang A, Qi R, Liu T, Yin D, Liu G. Nucleolin (NCL) inhibits the growth of peste des petits ruminants virus. *J Gen Virol*. 2020;101:33–43. <https://doi.org/10.1099/jgv.0.001358>.
48. Su PY, Wang YF, Huang SW, Lo YC, Wang YH, Wu SR, Shieh DB, Chen SH, Wang JR, Lai MD, Chang CF. Cell surface nucleolin facilitates enterovirus 71 binding and infection. *J Virol*. 2015;89:4527–38. <https://doi.org/10.1128/JVI.03498-14>.
49. Yan Y, Du Y, Wang G, Li K. Non-structural protein 1 of H3N2 influenza A virus induces nucleolar stress via interaction with nucleolin. *Sci Rep*. 2017;7:17761. <https://doi.org/10.1038/s41598-017-18087-2>.
50. Das S, Cong R, Shandilya J, Senapati P, Moindrot B, Monier K, Delage H, Mongelard F, Kumar S, Kundu TK, Bouvet P. Characterization of nucleolin K88 acetylation defines a new pool of nucleolin colocalizing with pre-mRNA splicing factors. *FEBS Lett*. 2013;587:417–24. <https://doi.org/10.1016/j.febslet.2013.01.035>.
51. Svinikina T, Gu H, Silva JC, Mertins P, Qiao J, Fereshetian S, Jaffe JD, Kuhn E, Udeshi ND, Carr SA. Deep, quantitative Coverage of the lysine Acetylome using Novel anti-acetyl-lysine antibodies and an optimized proteomic workflow. *Mol Cell Proteomics*. 2015;14:2429–40. <https://doi.org/10.1074/mcp.O114.047555>.
52. Pehar M, Ball LE, Sharma DR, Harlan BA, Comte-Walters S, Neely BA, Vargas MR. Changes in protein expression and lysine Acetylation Induced by decreased glutathione levels in astrocytes. *Mol Cell Proteomics*. 2016;15:493–505. <https://doi.org/10.1074/mcp.M115.049288>.
53. Kawaguchi A. [Dynamics of the influenza virus genome regulated by cellular host factors]. *Uirusu*. 2017;67:59–68. <https://doi.org/10.2222/jsv.67.59>.
54. Ganaie SS, Zou W, Xu P, Deng X, Kleiboeker S, Qiu J. Phosphorylated STAT5 directly facilitates parvovirus B19 DNA replication in human erythroid progenitors through interaction with the MCM complex. *PLoS Pathog*. 2017;13:e1006370. <https://doi.org/10.1371/journal.ppat.1006370>.
55. Dabral P, Uppal T, Rossetto CC, Verma SC. Minichromosome maintenance proteins cooperate with LANA during the G1/S phase of the cell cycle to support viral DNA replication. *J Virol*. 2019;93. <https://doi.org/10.1128/JVI.02256-18>.
56. Takei Y, Assenberg M, Tsujimoto G, Laskey R. The MCM3 acetylase MCM3AP inhibits initiation, but not elongation, of DNA replication via interaction with MCM3. *J Biol Chem*. 2002;277:43121–5. <https://doi.org/10.1074/jbc.C200442200>.
57. Jheng JR, Wang SC, Jheng CR, Horng JT. Enterovirus 71 induces dsRNA/PKR-dependent cytoplasmic redistribution of GRP78/BiP to promote viral replication. *Emerg Microbes Infect*. 2016;5:e23. <https://doi.org/10.1038/emi.2016.20>.
58. Montalbano R, Honrath B, Wisniewski TT, Elxnat M, Roth S, Ocker M, Quint K, Churin Y, Roederfeld M, Schroeder D, Glebe D, Roeb E, Di Fazio P. Exogenous hepatitis B virus envelope proteins induce endoplasmic reticulum stress: involvement of cannabinoid axis in liver cancer cells. *Oncotarget*. 2016;7:20312–23. <https://doi.org/10.18632/oncotarget.7950>.
59. Dekker C, Stirling PC, McCormack EA, Filmore H, Paul A, Brost RL, Costanzo M, Boone C, Leroux MR, Willison KR. The interaction network of the chaperonin CCT. *EMBO J*. 2008;27:1827–39. <https://doi.org/10.1038/emboj.2008.108>.
60. Yam AY, Xia Y, Lin HT, Burlingame A, Gerstein M, Frydman J. Defining the TRiC/CCT interactome links chaperonin function to stabilization of newly made proteins with complex topologies. *Nat Struct Mol Biol*. 2008;15:1255–62. <https://doi.org/10.1038/nsmb.1515>.
61. Pejanovic N, Hochrainer K, Liu T, Aerne BL, Soares MP, Anrather J. Regulation of nuclear factor kappaB (NF-kappaB) transcriptional activity via p65 acetylation by the chaperonin containing TCP1 (CCT). *PLoS ONE*. 2012;7:e42020. <https://doi.org/10.1371/journal.pone.0042020>.
62. Lin YF, Lee YF, Liang PH. Targeting beta-tubulin:CCT-beta complexes incurs Hsp90- and VCP-related protein degradation and induces ER stress-associated apoptosis by triggering capacitative Ca2+ entry, mitochondrial perturbation and caspase overactivation. *Cell Death Dis*. 2012;3:e434. <https://doi.org/10.1038/cddis.2012.173>.
63. Trinidad AG, Muller PA, Cuellar J, Klejnot M, Nobis M, Valpuesta JM, Voudsen KH. Interaction of p53 with the CCT complex promotes protein folding and wild-type p53 activity. *Mol Cell*. 2013;50:805–17. <https://doi.org/10.1016/j.molcel.2013.05.002>.
64. Yokota S, Yanagi H, Yura T, Kubota H. Cytosolic chaperonin is up-regulated during cell growth. Preferential expression and binding to tubulin at G1/S transition through early S phase. *J Biol Chem*. 1999;274:37070–8. <https://doi.org/10.1074/jbc.274.52.37070>.
65. Inoue Y, Aizaki H, Hara H, Matsuda M, Ando T, Shimoji T, Murakami K, Masaki T, Shoji I, Homma S, Matsuura Y, Miyamura T, Wakita T, Suzuki T. Chaperonin TRiC/CCT participates in replication of hepatitis C virus genome via interaction with the viral NS5B protein. *Virology*. 2011;410:38–47. <https://doi.org/10.1016/j.virol.2010.10.026>.
66. Zhang J, Wu X, Zan J, Wu Y, Ye C, Ruan X, Zhou J. Cellular chaperonin CCTgamma contributes to rabies virus replication during infection. *J Virol*. 2013;87:7608–21. <https://doi.org/10.1128/JVI.03186-12>.
67. Hafirassou ML, Meertens L, Umama-Diaz C, Labeau A, Dejarnac O, Bonnet-Madin L, Kummerer BM, Delaugerre C, Roingard P, Vidalain PO, Amara A. A Global Interactome Map of the Dengue Virus NS1 identifies virus restriction and dependency host factors. *Cell Rep*. 2018;22:1364. <https://doi.org/10.1016/j.celrep.2018.01.038>.
68. Knowlton JJ, Fernandez de Castro I, Ashbrook AW, Gestaut DR, Zamora PF, Bauer JA, Forrest JC, Frydman J, Risco C, Dermody TS. The TRiC chaperonin controls reovirus replication through outer-capsid folding. *Nat Microbiol*. 2018;3:481–93. <https://doi.org/10.1038/s41564-018-0122-x>.
69. Wang Q, Huang WR, Chih WY, Chuang KP, Chang CD, Wu Y, Huang Y, Liu HJ. Cdc20 and molecular chaperone CCT2 and CCT5 are required for the

- muscovy duck reovirus p10.8-induced cell cycle arrest and apoptosis. *Vet Microbiol.* 2019;235:151–63. <https://doi.org/10.1016/j.vetmic.2019.06.017>.
70. Luo H. Interplay between the virus and the ubiquitin-proteasome system: molecular mechanism of viral pathogenesis. *Curr Opin Virol.* 2016;17:1–10. <https://doi.org/10.1016/j.coviro.2015.09.005>.
71. Kong F, You H, Kong D, Zheng K, Tang R. The interaction of hepatitis B virus with the ubiquitin proteasome system in viral replication and associated pathogenesis. *Viol J.* 2019;16:73. <https://doi.org/10.1186/s12985-019-1183-z>.
72. Yeom S, Jeong H, Kim SS, Jang KL. Hepatitis B virus X protein activates proteasomal activator 28 gamma expression via upregulation of p53 levels to stimulate virus replication. *J Gen Virol.* 2018;99:655–66. <https://doi.org/10.1099/jgv.0.001054>.
73. Horwitz GA, Zhang K, McBrien MA, Grunstein M, Kurdistani SK, Berk AJ. Adenovirus small e1a alters global patterns of histone modification. *Science.* 2008;321:1084–5. <https://doi.org/10.1126/science.1155544>.
74. Suberbielle E, Stella A, Pont F, Monnet C, Mouton E, Lamouroux L, Monsarrat B, Gonzalez-Dunia D. Proteomic analysis reveals selective impediment of neuronal remodeling upon Borna disease virus infection. *J Virol.* 2008;82:12265–79. <https://doi.org/10.1128/JVI.01615-08>.
75. Hatakeyama D, Shoji M, Yamayoshi S, Yoh R, Ohmi N, Takenaka S, Saitoh A, Arakaki Y, Masuda A, Komatsu T, Nagano R, Nakano M, Noda T, Kawaoka Y, Kuzuhara T. Influenza A virus nucleoprotein is acetylated by histone acetyltransferases PCAF and GCN5. *J Biol Chem.* 2018;293:7126–38. <https://doi.org/10.1074/jbc.RA117.001683>.
76. Jiang G, Nguyen D, Archin NM, Yuki SA, Mendez-Lagares G, Tang Y, Elsheikh MM, Thompson GR 3rd, Connor H-O, Margolis DJ, Wong DM JK and, Dandekar S. HIV latency is reversed by ACS2-driven histone crotonylation. *J Clin Invest.* 2018;128:1190–8. <https://doi.org/10.1172/JCI98071>.
77. Hatakeyama D, Ohmi N, Saitoh A, Makiyama K, Morioka M, Okazaki H, Kuzuhara T. Acetylation of lysine residues in the recombinant nucleoprotein and VP40 matrix protein of Zaire Ebolavirus by eukaryotic histone acetyltransferases. *Biochem Biophys Res Commun.* 2018;504:635–40. <https://doi.org/10.1016/j.bbrc.2018.09.007>.
78. Zhu L, Jiang X, Fu X, Qi Y, Zhu G. The involvement of histone H3 acetylation in bovine herpesvirus 1 replication in MDBK cells. *Viruses.* 2018;10. <https://doi.org/10.3390/v10100525>.
79. Mantyla E, Salokas K, Oittinen M, Aho V, Mantysaari P, Palmujoki L, Kalliollinna O, Ihalainen TO, Niskanen EA, Timonen J, Viiri K, Vihinen-Ranta M. Promoter-targeted histone acetylation of Chromatinized Parvoviral Genome is essential for the progress of infection. *J Virol.* 2016;90:4059–66. <https://doi.org/10.1128/JVI.03160-15>.

Publisher's Note

Springer Nature remains neutral with regard to jurisdictional claims in published maps and institutional affiliations.